

# Coincidence Errors in a Cloud Droplet Probe (CDP) and a Cloud and Aerosol Spectrometer (CAS), and the Improved Performance of a Modified CDP

SARA LANCE

*Cooperative Institute for Research in Environmental Sciences, and National Oceanic and Atmospheric Administration, Boulder, Colorado*

(Manuscript received 18 November 2011, in final form 25 April 2012)

## ABSTRACT

Central to the aerosol indirect effect on climate is the relationship between cloud droplet concentrations  $N_d$  and cloud condensation nuclei (CCN) concentrations. There are valid reasons to expect a sublinear relationship between measured  $N_d$  and CCN, and such relationships have been observed for clouds in a variety of locations. However, a measurement artifact known as “coincidence” can also produce a sublinear trend. The current paper shows that two commonly used instruments, the cloud droplet probe (CDP) and the cloud and aerosol spectrometer (CAS), can be subject to significantly greater coincidence errors than are typically recognized, with an undercounting bias of at least 27% and an oversizing bias of 20%–30% on average at  $N_d = 500 \text{ cm}^{-3}$ , and with an undercounting bias of as much as 44% at  $N_d = 1000 \text{ cm}^{-3}$ . This type of systematic error may have serious implications for interpretation of in situ cloud observations. It is shown that a simple optical modification of the CDP dramatically reduces oversizing and undercounting biases due to coincidence. Guidance is provided for diagnosing coincidence errors in CAS and CDP instruments.

## 1. Introduction

### *a. Motivation*

The number concentration of droplets  $N_d$  formed in a warm ( $>0^\circ\text{C}$ ) cloud relies on the subset of the aerosol population known as cloud condensation nuclei (CCN), which exist as a function of the water vapor supersaturation  $S$ . Cloud supersaturations are dependent on the shape of the CCN activation spectrum [ $\text{CCN}(S)$ ] in addition to the cloud updraft velocity and/or radiative cooling rate (Twomey 1959). Therefore, even in the simplest case (adiabatic cores of nonprecipitating, liquid-only clouds), aerosol–cloud interactions are highly coupled, and the  $N_d$ –CCN relationship may be sublinear because of feedbacks with cloud water vapor. To be clear, sublinear in this context means that greater CCN leads to greater  $N_d$ , but at a diminishing rate as CCN increase. Limited droplet growth kinetics may play a role in this dynamic equilibrium, but it is unclear whether such an effect leads to greater or fewer droplets on average (Feingold and Chuang 2002; Nenes et al. 2002; Lance

et al. 2004). Processes such as entrainment mixing and droplet coagulation can also reduce  $N_d$  subsequent to cloud formation (Lehmann et al. 2009; Brenguier and Wood 2009), and such processes may be influenced by CCN concentrations as well (Albrecht 1989; Small et al. 2009; Hill et al. 2009). Many of the known processes act to dampen the effect of the initial aerosol perturbation (Stevens and Feingold 2009). Therefore, it is not surprising that a variety of sublinear relationships between measured  $N_d$  and CCN have been observed, with measured  $N_d$  often limited to  $<400 \text{ cm}^{-3}$  even in polluted environments with  $\text{CCN}(S = 0.5\%)$  as high as  $1000 \text{ cm}^{-3}$  (Gultepe and Isaac 1999; Chuang et al. 2000; Ramanathan et al. 2001b,a; Rosenfeld et al. 2008a,b; Twohy et al. 2005; Feng and Ramanathan 2010; Kleinman et al. 2011).

However, a measurement artifact known as “coincidence,” if not accounted for, can also produce a sublinear trend between  $N_d$  and CCN. Coincidence events occur when more than one droplet is registered by an instrument at the same time (Baumgardner et al. 1985; Cooper 1988), resulting in multiple droplets artificially measured as one droplet, which leads to a tailing off of measured droplet concentrations as actual concentrations increase (Brenguier et al. 1994; Burnet and Brenguier 2002). In addition to an undercounting bias, coincidence often results in oversizing bias and significant broadening of the measured

---

*Corresponding author address:* Sara Lance, David Skaggs Research Center, 325 Broadway, Mailstop R/CSD2, Boulder, CO 80305.

E-mail: sara.m.lance@noaa.gov

droplet size distribution, which exacerbates the issue because undercounting bias and oversizing bias both suggest that the cloud is less polluted than it is.

The current study follows from that by Lance et al. (2010), in which it was determined, based on laboratory calibrations with single water droplets and Monte Carlo simulations, that a commonly used instrument known as the cloud droplet probe (CDP) may realistically suffer from as much as 25% undercounting error and 30% oversizing error due to coincidence at  $N_d$  as low as  $200 \text{ cm}^{-3}$ . For the current study, observations from the California Nexus (CalNex) 2010 campaign are used to clearly demonstrate that in situ CDP measurements are strongly affected by coincidence errors and also to show that a simple optical modification can dramatically reduce those coincidence errors. The current study also demonstrates that another commonly used instrument known as the cloud and aerosol spectrometer (CAS) can be subject to coincidence errors as great as the CDP, even though a CAS has been used previously in successful droplet closure experiments in polluted environments with  $N_d$  as high as  $1200 \text{ cm}^{-3}$  with only minor coincidence corrections applied (Conant et al. 2004; Meskhidze et al. 2005).

The primary result of this paper is to show that, even though current cloud probe instruments typically have much faster electronics than instruments from 20 years ago (thereby preventing errors related to electronic deadtime), optical coincidence can still be an important issue. Furthermore, the coincidence error is dependent on more than simply the qualified sample area; the area viewable by only the sizing detector can affect the counting rate as well, and this type of “extended coincidence” is the dominant error for the observations shown here (Baumgardner et al. 1985; Lance et al. 2010). Failing to account for the systematic measurement bias from coincidence events may result in serious underestimation of the aerosol effect on clouds, or overestimation of processes that act to buffer cloud systems, such as those described by Stevens and Feingold (2009).

### *b. Clouds and coincidence during the CalNex 2010 campaign*

The CalNex 2010 campaign took place in and near California (<http://www.esrl.noaa.gov/csd/calnex/>) on May–June 2010. Observations from eight flights during the CalNex 2010 project (12, 14, 16, and 31 May and 2, 3, 16, and 18 June) are reported in this paper, spanning 135 min of in-cloud measurements. These marine stratocumulus clouds were typically intercepted just offshore, at locations ranging from the Los Angeles Bight to as far north as Monterey.

The campaign was designed for evaluating emissions, transport, and chemical processes relevant for climate

change and air quality considerations. Boundary layer marine stratus clouds, which are persistent near the California coast during this time of year, have an important role to play in processes affecting both climate and air quality. Investigating interactions between pollution and clouds was therefore one goal of the CalNex campaign, and polluted clouds were specifically targeted.

Clouds can have an important impact on aerosol properties and transport of pollutants. Although clouds can clean the atmosphere by wet scavenging of aerosol pollution, clouds can also enhance the boundary layer temperature inversion, thereby stabilizing concentrated pollution plumes above cloud top (Brioude et al. 2009). Cloud droplets, with typically more than an order of magnitude greater surface area than deliquesced aerosol, may participate in chemical reactions that result in modified aerosol and gas phase composition (Sorooshian et al. 2007; Hennigan et al. 2008) and aerosol size (Hoppel et al. 1994). Clouds may also impact new particle formation rates because of enhanced photolytic activity, depleted aerosol surface area, and transport of aerosol precursor gases into cloud outflow regions (Clarke et al. 1999; Weber et al. 2001; Holmes 2007; Kazil et al. 2011).

The effect of aerosols on clouds is also important and remains the most uncertain climate forcing. In addition to increased cloud albedo resulting from greater CCN concentrations for a given cloud liquid water content (LWC) (Twomey 1959), initiation of precipitation within marine boundary layer clouds may be inhibited by greater CCN concentrations (Albrecht 1989; Brenguier and Wood 2009). Changes to the onset or intensity of precipitation can affect both the radiative balance and the hydrological cycle, with important implications for the incidence and severity of drought, wildfires, and mudslides in California.

Study of these different cloud processes relies on accurate measurements of cloud droplet size distributions, for which in situ measurements are expected to be the most accurate. Understanding the influence of aerosol properties on cloud formation requires accurate measurement of cloud droplet number concentrations, understanding the influence of clouds on heterogeneous reactions requires accurate measurement of cloud droplet surface area, and understanding the initiation of precipitation requires accurate measurement of cloud droplet mass distributions. Each of these measured parameters is influenced differently by coincidence artifacts.

## **2. Methods**

Cloud droplets 3–50  $\mu\text{m}$  in diameter were measured simultaneously with three instruments during CalNex 2010, as defined in Table 1. In total, five cloud probes

TABLE 1. Cloud instruments on board the NOAA WP-3D during CalNex 2010.

Instrument name	Acronym	Measurement method	Nominal range	Units
Cloud and aerosol spectrometer (Serial No. CAS-0708-017)	CAS	Forward/back scattering	0.6–50	$\mu\text{m}$
Modified cloud droplet probe (Serial No. CCP-0703-010)	M-CDP	Forward scattering	3–50	$\mu\text{m}$
Standard cloud droplet probe (Serial No. CCP-0703-009)	S-CDP	Forward scattering	3–50	$\mu\text{m}$
Modified cloud imaging probe (Serial No. CCP-0703-009)	M-CIP	2D shadow image	25–2000	$\mu\text{m}$
Standard cloud imaging probe (Serial No. CCP-0703-010)	S-CIP	2D shadow image	25–2000	$\mu\text{m}$
CSIRO King probe	King-LWC	Hot wire (1.87 mm)	0.02–5.0	$\text{g m}^{-3}$
SEA multiprobe	SEA-LWC1	Hot wire (0.533 mm)		
	SEA-LWC2	Hot wire (2.108 mm)		
	SEA-TWC	Heated trough		

manufactured by Droplet Measurement Technologies, Inc. (DMT) operated simultaneously from beneath the portside wing of the National Oceanic and Atmospheric Administration (NOAA) Lockheed WP-3D Orion (WP-3D) aircraft (Fig. 1).

The nomenclature used here follows that detailed by Lance et al. (2010). Qualified droplets are those that transit across a small region of the laser beam defined as the qualified sample area ( $SA_Q$ ), where light scattered by a droplet is simultaneously detected with sufficient signal by two photodetectors known as a “qualifier” and a “sizer.” Unqualified droplets are those that transit across the laser beam in a region outside of  $SA_Q$  but are often still detected by the sizer, in a region defined as the extended sample area ( $SA_E$ ). To reduce extended coincidence errors for the modified CDP (M-CDP), an 800- $\mu\text{m}$ -diameter pinhole was installed directly in front of the sizing detector. The qualifier and sizer response within  $SA_Q$  and  $SA_E$  were calibrated with a stream of single water droplets prior to the Calnex 2010 campaign for the M-CDP and the standard CDP (S-CDP) using the procedure described by Lance et al. (2010). Figure 2 shows the normalized sizing detector response to 20- $\mu\text{m}$  water droplets transmitted across the CDP laser beam at different lateral and longitudinal positions. As a result of the added pinhole,  $SA_E$  for the M-CDP is reduced by  $\sim 8$  times (2.7 instead of 20.5  $\text{mm}^2$ ). However,  $SA_Q$ , the area within which droplets are actually counted remains unaffected. The pinhole, therefore, is a simple optical modification that reduces extended coincidence errors without limiting the measurement counting statistics.

The calibrations with water droplets reveal that there can be significant variability between the same model instrument, illustrating the need for such calibrations. For instance,  $SA_Q$  is slightly different between the probes (Table 2). Also,  $SA_E$  for the S-CDP is 16.8  $\text{mm}^2$ , which is  $\sim 20\%$  smaller than for the standard CDP used during Aerosol, Radiation, and Cloud Processes affecting Arctic Climate (ARCPAC) 2008 (this instrument was described in detail by Lance et al. 2010).

The CAS sizing response was calibrated with polystyrene latex spheres and glass beads during CalNex 2010. Calibrations with water droplets were not obtained for the CAS, since the sample area of the CAS is not accessible enough for obtaining independent droplet sizing with a microscope, as done in the CDP calibrations. Because of this limitation,  $SA_E$  and  $SA_Q$  for the CAS were also not calibrated. Instead,  $SA_Q$  was determined during postprocessing of the CalNex dataset by comparing the CAS observations with the CDP observations. During CalNex 2010, the M-CDP sampled at a rate of 10 Hz, while the S-CDP, CAS, and both CIPs sampled at 1 Hz because of data transfer limitations.

Bulk LWC was measured at 1 Hz with a Commonwealth Scientific and Industrial Research Organisation (CSIRO) King probe (King-LWC) and at 10 Hz with a Scientific Engineering Applications (SEA) multiprobe, which contained two heated cylindrical wires of approximately 0.5- and 2.1-mm diameter and a 4-mm-wide “trough shaped” sensor intended to measure total water content (SEA-TWC) of both frozen and liquid particles (Lilie et al. 2004). For direct comparisons, measurements made at 10 Hz are averaged to 1 Hz. Comparisons



FIG. 1. Cloud probe instruments used during CalNex, labeled by acronyms as defined in Table 1. Wingtip location is toward the right. Another NOAA WP-3D aircraft is visible in the background of the image.

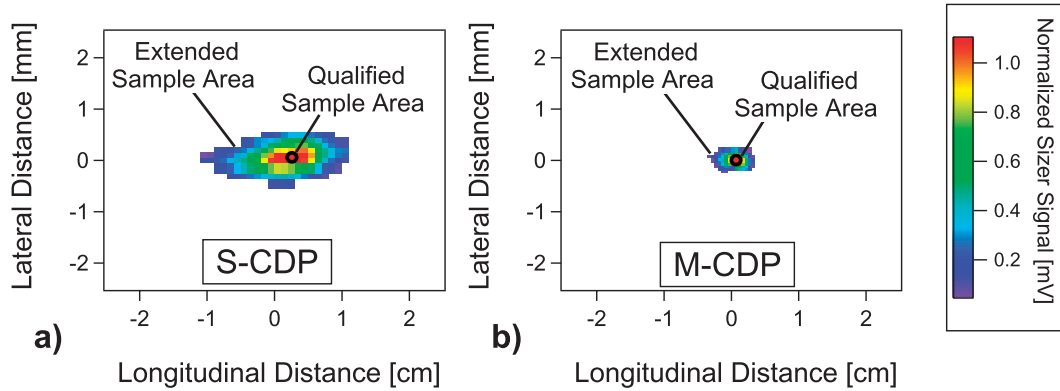


FIG. 2. Calibration of the extended sample area, obtained by transmitting water droplets 20–24  $\mu\text{m}$  in diameter at precise locations across the laser beam of (a) a standard CDP and (b) a CDP that has been modified by adding a pinhole to the sizing detector. The color represents the normalized sizing detector response.

between droplet concentration and size measured by the CAS and the two CDPs are explored. CDP-LWC (obtained by integrating the measured droplet size distributions) is also compared with LWC measured from the bulk LWC probes. Together, these independently derived cloud microphysical observations provide a robust test of the performance of these instruments. Note that none of the measurements have been modified to account for possible coincidence artifacts, as the magnitude of coincidence errors is precisely what we would like to determine. In the following analysis, measurements made by the M-CDP are denoted with an asterisk to distinguish from the S-CDP measurements (e.g., CDP-LWC\* refers to the LWC derived from the droplet size distribution measured by the M-CDP, whereas CDP-LWC refers to the same as measured by the S-CDP).

### 3. Results

Direct comparison between the cloud probe measurements during CalNex 2010 show that the S-CDP systematically counts fewer droplets relative to the M-CDP, and the magnitude of this discrepancy increases with droplet concentrations, as expected for greater undercounting bias due to coincidence by the S-CDP. Droplet concentrations  $N_d$  measured by the S-CDP relative to droplet concentrations  $N_d^*$  measured by the M-CDP are shown in Fig. 3a, colored by the volume mean diameter  $D_v^*$  derived from the M-CDP measurements. The observations shown in Fig. 3a are fit to an exponential equation of the form

$$N_d^* = A(\exp^{BN_d} - 1), \quad (1)$$

where  $A = 749.7 \text{ cm}^{-3}$  and  $B = 1.4254 \times 10^{-3} \text{ cm}^3$ . Assuming that no undercounting due to coincidence

occurs in the M-CDP, the concentration bias of the S-CDP relative to actual droplet concentrations is  $-27\%$  at  $N_d^* = 500 \text{ cm}^{-3}$  and  $-44\%$  at  $N_d^* = 1000 \text{ cm}^{-3}$ . The simulated performance of the standard CDP operated during ARCPAC 2008 (Lance et al. 2010) is also shown in Figs. 3a,b for comparison to the observations from CalNex 2010. The current observations confirm the magnitude of undercounting errors predicted in the previous study. The reduced undercounting error for the observations is consistent with the fact that  $SA_E$  is  $\sim 20\%$  smaller for the S-CDP operated during CalNex 2010 than the CDP operated during ARCPAC 2008.

In addition to undercounting droplets, coincidence events are expected to result in an oversizing bias since coincident droplets scatter more light than a single droplet of the same size. The observations shown in Fig. 3b confirm this prediction; droplets measured by the S-CDP are larger than those measured by the M-CDP, and the oversizing bias increases with droplet concentrations. Furthermore, smaller droplets experience greater oversizing error than larger droplets, as expected because of the nonlinear relationship between sizing detector voltage and droplet size, as discussed in more detail by Lance et al. (2010).

The average transit time  $t_{\text{avg}}$  provides a diagnostic of coincidence errors (Lance et al. 2010). Observations during CalNex 2010 show that  $t_{\text{avg}}$  increases with  $N_d^*$

TABLE 2. Qualified and extended sample areas, determined by micropositioning 20–24- $\mu\text{m}$  water droplets.

Instrument	$SA_Q$ ( $\text{mm}^2$ )	$SA_E$ ( $\text{mm}^2$ )
M-CDP	$0.3 \pm 0.04$	$2.7 \pm 0.04$
S-CDP	$0.26 \pm 0.05$	$16.8 \pm 0.04$
CAS	$0.6^*$	

\* Estimated CAS qualified sample area based on comparison with CDP measurements during CalNex 2010.

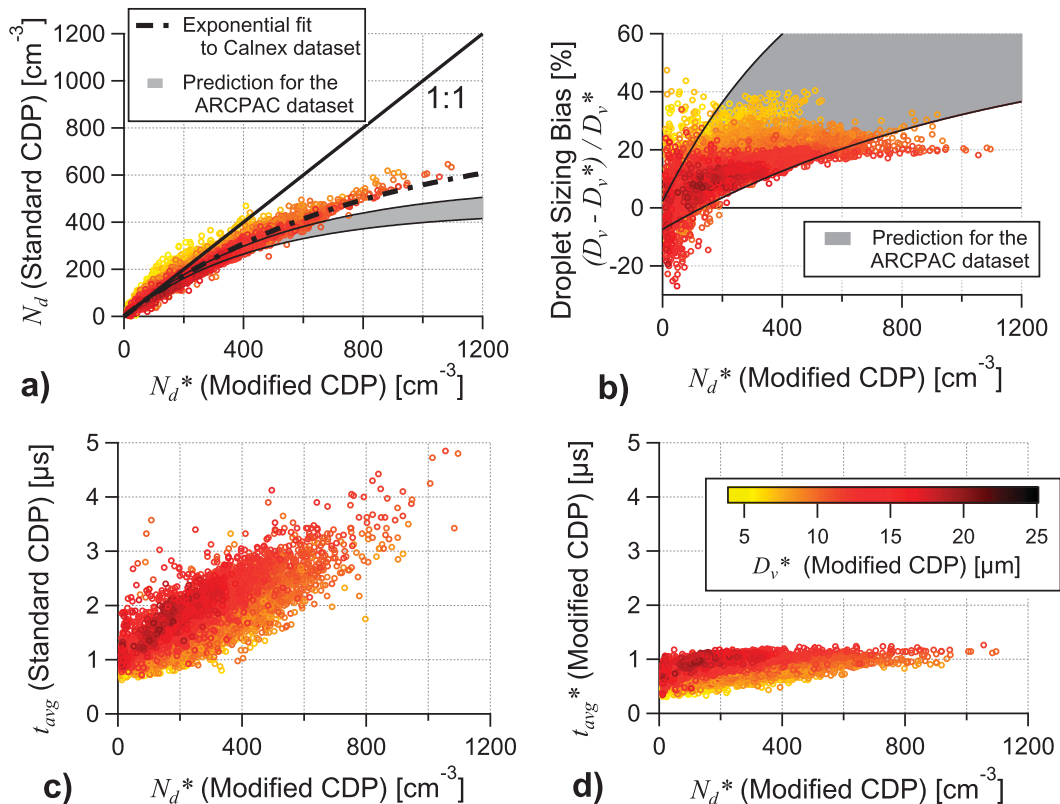


FIG. 3. Direct comparison between S-CDP and M-CDP measurements during the CalNex campaign. Plotted vs M-CDP droplet concentrations are (a) S-CDP droplet concentrations, (b) percent bias in volume mean diameter for the S-CDP compared to the M-CDP, (c) average transit time for the S-CDP, and (d) average transit time for the M-CDP. Markers are colored by the volume mean diameter  $D_v^*$ . Also shown is the range of predictions from Lance et al. (2010) for the standard CDP used during ARCPAC 2008, based on Monte Carlo simulations and detailed laboratory calibrations of the instrument response.

(Fig. 3d) while  $t_{avg}^*$  remains relatively flat as  $N_d^*$  increases (Fig. 3c), reflecting the reduced coincidence artifacts experienced by the M-CDP.

An example time series of measurements from the 14 May flight during CalNex 2010 (Fig. 4) shows that the M-CDP records both higher droplet concentrations ( $N_d^* > N_d$ ) and smaller droplet sizes (as evidenced by the fact that  $CDP-LWC^* < CDP-LWC$ ) than the S-CDP. Again, undercounting and oversizing together exhibit the expected biases resulting from extended coincidence errors in the S-CDP. During the  $\sim 3$  min for this example the S-CDP shows an average undercounting bias of 28% and oversizing bias of 24% relative to the M-CDP. Comparison to bulk LWC measurements reaffirms our expectation that the differences in the M-CDP and S-CDP observations are largely due to coincidence errors. For this example time series we see that  $CDP-LWC^*$  agrees well with both King-LWC and SEA-TWC, while  $CDP-LWC$  is clearly greater than the other three measurements. Comparison to bulk LWC measurements also suggests that the M-CDP suffers from nonnegligible

oversizing due to coincidence errors at high droplet concentrations; note in Fig. 4 that when  $N_d^* > \sim 600$  cm<sup>-3</sup>,  $CDP-LWC^*$  is as much as 40% greater than bulk LWC measurements.

Comparisons of the CDP-LWC to bulk LWC measurements for all cloud flights during CalNex 2010 are shown in Fig. 5. The best agreement between these four instruments is between the M-CDP and the SEA TWC probes (Fig. 5d). The agreement between the M-CDP and King LWC probe is also good when  $D_v^* < 20$   $\mu$ m (Fig. 5b). The fact that King-LWC  $<$  SEA-TWC for drops with  $D_v^* < 20$   $\mu$ m suggests that drop retention after collision with the hot-wire probes is  $< 100\%$  for larger drops. Splattering of large droplets upon impact on the King-LWC probe has been shown in wind tunnel studies to reduce instrument response for droplets as small as  $\sim 20$ – $30$   $\mu$ m at velocities of 60–100 m s<sup>-1</sup> (Biter et al. 1987; Strapp et al. 2003). The trough-shaped design of the SEA TWC probe was chosen primarily for its efficiency to collect ice particles (Lilie et al. 2004), but an additional benefit of this design is likely better collection

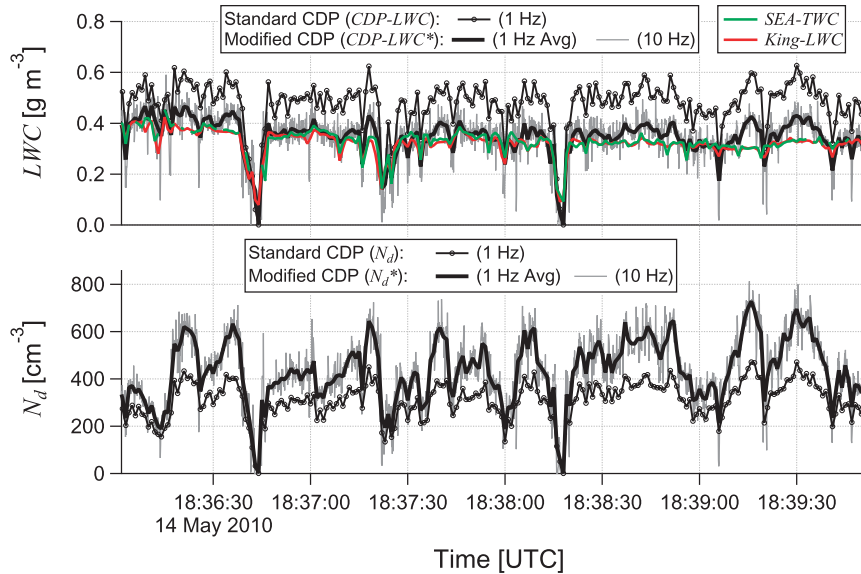


FIG. 4. Time series of S-CDP and M-CDP measurements obtained during a flight on 14 May 2010 in marine stratus off the coast of Los Angeles, California, during CalNex 2010. Coincidence results in undercounting and oversizing errors; the M-CDP experiences much less of both. (top) CDP-LWC\* obtained from M-CDP measurements agrees much better with bulk LWC measurements as plotted in color.

efficiency for large liquid droplets compared to hot-wire probes, similar to the improved response of the Nevzorov TWC probe demonstrated by Strapp et al. (2003). Although the size-dependent response of the SEA TWC probe is not known, the excellent agreement between CDP-LWC\* and SEA-TWC for all droplet sizes indicates that both the M-CDP and SEA TWC probe were not subject to major biases for the clouds encountered during CalNex 2010, since it is unlikely that biases in one instrument will happen to exactly equal biases in the other instrument, especially given the very different measurement techniques.

Figures 5a and 5c show that CDP-LWC is almost always greater than both King-LWC and SEA-TWC. In the absence of additional information, one might reasonably suspect from these observations that the S-CDP simply suffers from a moderate sizing error (in this case, 1–2 size bins) or an overcounting bias (Figs. 5a,c). On average, a 10%–20% error in droplet sizing could account for the bias between measurements, which is realistically within the sizing uncertainty of CDP instruments, especially when calibrated with glass bead particles only (Lance et al. 2010). However, the CDP-LWC bias (relative to SEA-TWC) plotted as a function of  $N_d$  (Fig. 6) clearly demonstrates that the oversizing bias is due to coincidence. Oversizing on average leads to 90% bias in CDP-LWC at  $N_d$  of  $400 \text{ cm}^{-3}$  and only 10% bias in CDP-LWC at  $N_d$  of  $100 \text{ cm}^{-3}$ . Undercounting does not strongly affect the slope of this relationship,

since droplet concentrations are proportional to both axes. Note that a linear fit to the S-CDP observations gives a slope of  $25\% (100 \text{ cm}^{-3})^{-1}$  (Fig. 6a), which agrees very well to that observed for liquid-only clouds during ARCPAC 2008 using a different standard CDP probe (Lance et al. 2010). In contrast, a linear fit to the M-CDP observations gives a slope of  $7\% (100 \text{ cm}^{-3})^{-1}$  (Fig. 6b). For these calculations the data has been filtered for SEA-TWC  $> 0.1 \text{ g m}^{-3}$  to reduce noise.

Another important observation during CalNex 2010 is that the CAS suffered coincidence errors even greater than the S-CDP (Fig. 7). For  $N_d^* = 800 \text{ cm}^{-3}$ , droplet concentrations measured by the CAS are only  $370\text{--}550 \text{ cm}^{-3}$ , with on average  $>40\%$  undercounting bias. Figure 7a shows that for most of the CalNex 2010 cloud flights, undercounting by the CAS is consistent with the undercounting errors predicted for the unmodified CDP operated during ARCPAC 2008 (gray shaded area), as reported by Lance et al. (2010). The 2 June observations stand out as having apparently lesser undercounting errors for the CAS compared to the other flights. Note that the concentration of interstitial aerosol particles  $0.6\text{--}3 \mu\text{m}$  (also measured by the CAS) often exceeds  $200 \text{ cm}^{-3}$  on the 2 June flight, which also distinguishes this flight from the others (Fig. 7b). For  $N_d^* = 800 \text{ cm}^{-3}$  the average undercounting error for the CAS is 37.5% on the 2 June flight, bringing the trend in closer agreement with the S-CDP observations during CalNex 2010 (dotted line), whereas the average

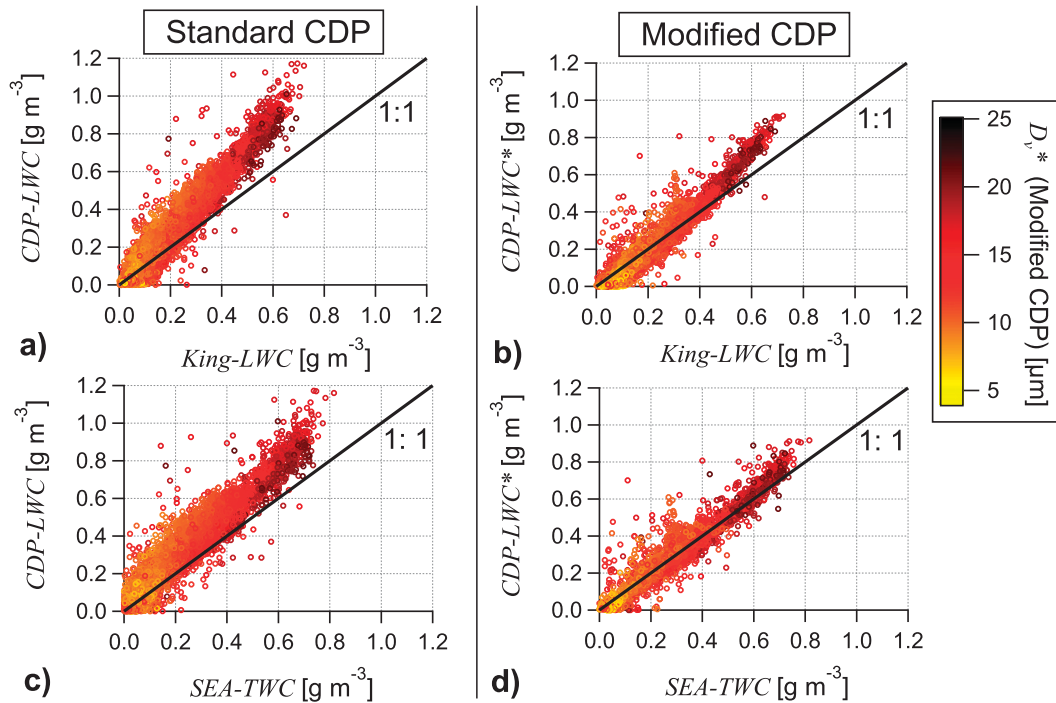


FIG. 5. Comparison of cloud water content between four instruments: the S-CDP (CDP-LWC), the M-CDP (CDP-LWC\*), the King probe (King-LWC), and the SEA probe (SEA-TWC). Markers are colored by the volume mean diameter  $D_v^*$ .

undercounting error for the CAS on all other flights is 49% at  $N_d^* = 800 \text{ cm}^{-3}$ . A shift in the measured size distribution may explain why the 2 June flight is different from the other flights; at high interstitial aerosol loadings, some of the interstitial particles transit across  $SA_E$  and  $SA_Q$  at the same time and may be counted as a single small droplet (defined here as a particle with diameter  $> 3 \mu\text{m}$ ). In this case we see that an oversizing

bias due to coincidence can partially compensate for an undercounting bias due to coincidence.

#### 4. Discussion

The CAS undercounting error observed during CalNex 2010 strongly contrasts statements made by Conant et al. (2004), where successful cloud droplet

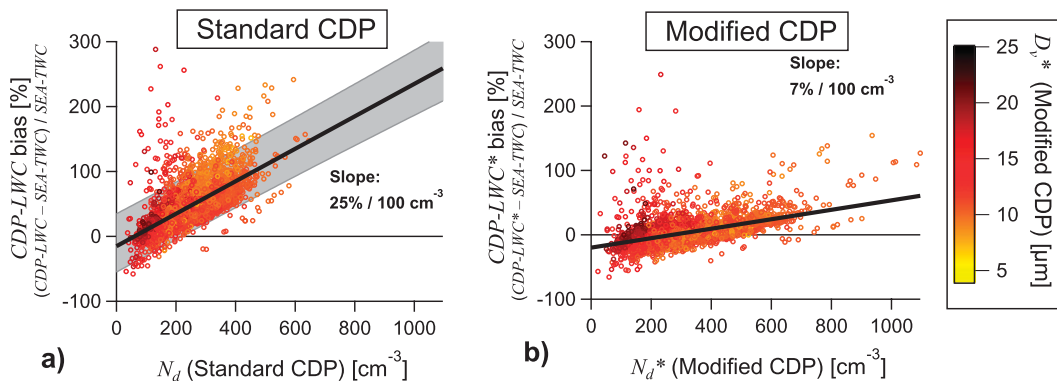


FIG. 6. Measured CDP-LWC bias relative to SEA-TWC for the (a) S-CDP and (b) M-CDP vs measured droplet concentrations. To reduce noise, measurements at CDP-LWC  $< 0.1 \text{ g m}^{-3}$  and SEA-TWC  $< 0.1 \text{ g m}^{-3}$  are not shown. Markers are colored by the volume mean diameter  $D_v^*$ . The gray shaded area shows the range of CDP measurements compared to King LWC observations from the ARCPAC 2008 campaign (at the 95% confidence level).

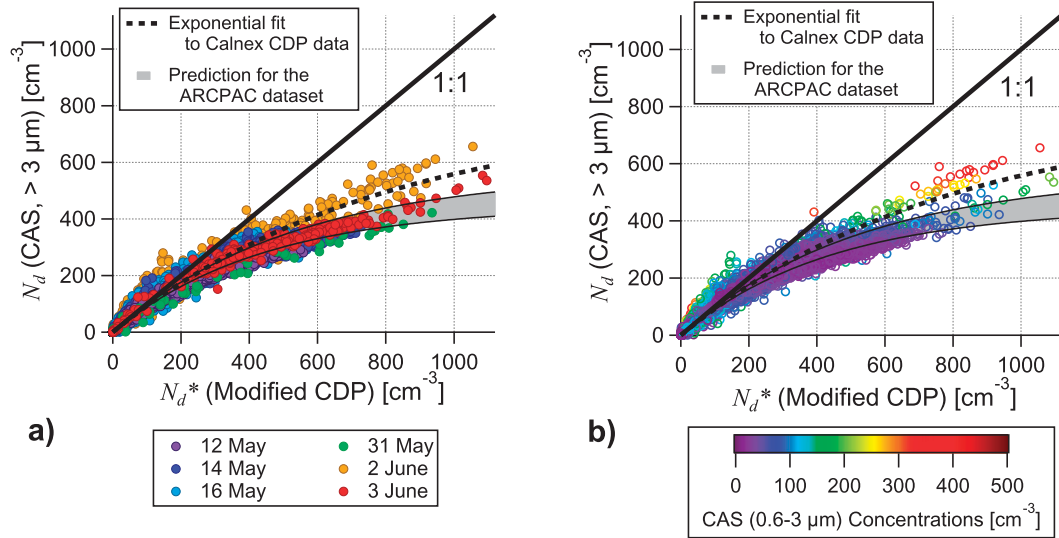


FIG. 7. Droplet concentrations measured by the CAS compared to the M-CDP, with (a) markers colored by flight and (b) markers colored by large aerosol ( $0.6\text{--}3 \mu\text{m}$ ) concentrations measured by the CAS. Shown for comparison is the exponential fit to the S-CDP measurements during CalNex 2010 and the simulated concentration bias of the standard CDP used during ARCPAC 2008.

closure was attained using CAS observations with minimal correction for coincidence artifacts:

Coincidence errors, which are typical of single particle optical probes (Baumgardner et al. 1985; Burnet and Brenguier 2002), are estimated to decrease cloud drop concentrations by 1% at  $800 \text{ cm}^{-3}$  and 10% at  $7000 \text{ cm}^{-3}$ .

As the following calculations show, the undercounting bias due to coincidence estimated above by Conant et al. (2004) appears to only consider standard coincidence events (resulting from coincident droplets transiting only through  $\text{SA}_Q$ ). The droplet concentration that is counted,  $N_c$ , can be estimated as  $N_c = N_a(1 - A)$  (Burnet and Brenguier 2002), where  $A$  is the instrument activity (the sum of electronic pulse widths per sampling interval, if electronic delays can be neglected) and where  $N_a$  is the actual droplet concentration. Here  $A$  can be estimated by multiplying the average pulse width by  $\lambda$  ( $\text{s}^{-1}$ ), the rate that droplets transit through  $\text{SA}_Q$ . Neglecting the effect of droplet size, the average pulse width can be estimated as  $w/V$ , where  $w$  is the beamwidth parallel to the airflow and  $V$  is the velocity of the droplet relative to the laser beam (or the aircraft true airspeed). Therefore,  $A \sim \lambda w/V$ , which simplifies to  $A \sim N_a \text{SA}_Q w$ , since  $\lambda = N_a \text{SA}_Q V$ . With  $\text{SA}_Q = 0.112 \text{ mm}^2$  and  $w = 0.1 \text{ mm}$  given by Conant et al. (2004), this simple calculation results in 0.9% undercounting error at  $N_a = 800 \text{ cm}^{-3}$  and 8.4% at  $N_a = 7000 \text{ cm}^{-3}$  because of standard coincidence only, which is comparable to the estimate from Conant et al. (2004).

As discovered through Monte Carlo simulations by Lance et al. (2010), extended coincidence events (resulting from coincident droplets transiting through  $\text{SA}_Q$  and  $\text{SA}_E$ ) dominate the coincidence errors, since  $\text{SA}_E \gg \text{SA}_Q$ . An important distinction between standard coincidence and extended coincidence errors is that the former always results in undercounting (since all droplets transiting through  $\text{SA}_Q$  should be counted) whereas the latter only results in undercounting when the coincident droplet(s) raise the sizer signal above the qualifier signal. Therefore,  $\text{SA}_E$  cannot simply replace  $\text{SA}_Q$  in the equation above to estimate undercounting errors because of extended coincidence events.

In the current study  $\text{SA}_E$  for the CAS used is apparently as large as  $\text{SA}_E$  for the S-CDP, since both instruments exhibit the same magnitude of undercounting compared to the M-CDP. It may be that some versions of the CAS or the CDP have historically had an aperture installed on the sizing detector to limit coincidence errors, which would explain the Conant et al. (2004) results. Ultimately, it is the responsibility of each researcher to ensure that they understand the performance of their own instrument and to be aware of potential systematic biases such as oversizing and undercounting errors due to coincidence. Researchers should be particularly vigilant when interpreting the shape of droplet size distributions or when estimating the magnitude of atmospheric processes based on measured droplet concentrations, as demonstrated by Cooper (1988).

To diagnose coincidence errors, the following steps can be taken: 1) Compare CDP-LWC to an independent bulk LWC measurement and plot this measurement bias as a function of measured droplet concentrations. 2) Record and plot average transit time (or pulse durations for a sampling of individual droplets) as a function of measured droplet concentrations. 3) Measure  $SA_E$  and  $SA_Q$  directly, as done in Lance et al. (2010). 4) Record the number of rejected pulses (which register on the sizing detector but not the qualifier) for comparison to the number of accepted pulses (which are registered by both detectors). The slope of this relationship will give an independent estimate for  $(SA_E - SA_Q)/SA_Q$ , but only at relatively low concentrations when all rejected pulses are recorded (rejected pulses are subject to undercounting due to coincidence, just like qualified pulses). 5) Record the full waveforms of photodetector pulses, for at least of subset of the measured droplets. In this way coincidence can be monitored more directly, because the shape of the pulses is affected by coincidence.

Note that the alignment of the M-CDP was consistent during the entire CalNex 2010 campaign. However, the alignment changed during shipping after the campaign, which resulted in substantial sizing and counting errors when calibrated with a jet of single water droplets in the laboratory after the campaign. It is likely that installation of a pinhole mask on the sizing detector makes the CAS and the CDP more prone to misalignment. The importance of accurate sizing and counting of droplets must be weighed against the added practical difficulties of maintaining alignment between the qualified and extended sample areas.

## 5. Summary and conclusions

Despite improved electronic response times and small sample areas, coincidence errors were found to be significant for the CDP and the CAS. At ambient droplet concentrations of  $500 \text{ cm}^{-3}$ , at least 27% undercounting and 20%–30% oversizing bias were observed, which is consistent with Monte Carlo simulations based on calibrated instrument response. Extended coincidence events, a consequence of the large area seen by the sizing detector, dominate the coincidence errors. In this paper, a simple optical modification of the CDP that consists of adding a pinhole to the sizing detector dramatically reduces this type of coincidence errors. The observations in this and in a previous study (Lance et al. 2010) show that this problem is not confined to the performance of an individual instrument. In fact, all three of the instruments tested have shown a strikingly similar performance with undercounting errors comparable to standard

(uncorrected) forward scatter spectrometer probes (FSSP-100) (Burnet and Brenguier 2002). Several methods for diagnosing coincidence errors are presented.

*Acknowledgments.* This work was supported by the National Oceanic and Atmospheric Administration (NOAA) climate and air quality programs. Thanks to DMT for their laboratory support in modifying the CDP. Thanks to Jorge Delgado and the NOAA Aircraft Operations Center for allowing use of their equipment and for technical support in the field. Special thanks to Charles Brock and Jan Kazil for helpful advice and editing of the manuscript.

## REFERENCES

- Albrecht, B. A., 1989: Aerosols, cloud microphysics, and fractional cloudiness. *Science*, **245**, 1227–1230.
- Baumgardner, D., W. Strapp, and J. E. Dye, 1985: Evaluation of the forward scattering spectrometer probe. Part II: Corrections for coincidence and dead-time losses. *J. Atmos. Oceanic Technol.*, **2**, 626–632.
- Biter, C. J., J. E. Dye, D. Huffman, and W. D. King, 1987: Drop-size response of the CSIRO liquid water probe. *J. Atmos. Oceanic Technol.*, **4**, 359–367.
- Brenguier, J. L., and R. Wood, 2009: Observational strategies from the micro- to mesoscale. *Clouds in the Perturbed Climate System: Their Relationship to Energy Balance, Atmospheric Dynamics, and Precipitation*, J. Heintzenberg and R. J. Charlson, Eds., The MIT Press, 487–510.
- , D. Baumgardner, and B. Baker, 1994: A review and discussion of processing algorithms for FSSP concentration measurements. *J. Atmos. Oceanic Technol.*, **11**, 1409–1414.
- Brioude, J., and Coauthors, 2009: Effect of biomass burning on marine stratocumulus clouds off the California coast. *Atmos. Chem. Phys.*, **9**, 8840–8856.
- Burnet, F., and J. L. Brenguier, 2002: Comparison between standard and modified forward scattering spectrometer probes during the Small Cumulus Microphysics Study. *J. Atmos. Oceanic Technol.*, **19**, 1516–1531.
- Chuang, P. Y., D. R. Collins, H. Pawlowska, J. R. Snider, H. H. Jonsson, J. L. Brenguier, R. C. Flagan, and J. H. Seinfeld, 2000: CCN measurements during ACE-2 and their relationship to cloud microphysical properties. *Tellus*, **52**, 843–867.
- Clarke, A. D., V. N. Kapustin, F. L. Eisele, R. J. Weber, and P. H. McMurry, 1999: Particle production near marine clouds: Sulfuric acid and predictions from classical binary nucleation. *Geophys. Res. Lett.*, **26**, 2425–2428.
- Conant, W. C., and Coauthors, 2004: Aerosol–cloud drop concentration closure in warm cumulus. *J. Geophys. Res.*, **109**, D13204, doi:10.1029/2003JD004324.
- Cooper, W. A., 1988: Effects of coincidence on measurements with a forward scattering spectrometer probe. *J. Atmos. Oceanic Technol.*, **5**, 823–832.
- Feingold, G., and P. Y. Chuang, 2002: Analysis of the influence of film-forming compounds on droplet growth: Implications for cloud microphysical processes and climate. *J. Atmos. Sci.*, **59**, 2006–2018.
- Feng, Y., and V. Ramanathan, 2010: Investigation of aerosol–cloud interactions using a chemical transport model constrained by satellite observations. *Tellus*, **62**, 69–86.

- Gultepe, I., and G. A. Isaac, 1999: Scale effects on averaging of cloud droplet and aerosol number concentrations: Observations and models. *J. Climate*, **12**, 1268–1279.
- Hennigan, C. J., M. H. Bergin, J. E. Dibb, and R. J. Weber, 2008: Enhanced secondary organic aerosol formation due to water uptake by fine particles. *Geophys. Res. Lett.*, **35**, L18801, doi:10.1029/2008GL035046.
- Hill, A. A., G. Feingold, and H. Jiang, 2009: The influence of entrainment and mixing assumption on aerosol–cloud interactions in marine stratocumulus. *J. Atmos. Sci.*, **66**, 1450–1464.
- Holmes, N. S., 2007: A review of particle formation events and growth in the atmosphere in the various environments and discussion of mechanistic implications. *Atmos. Environ.*, **41**, 2183–2201.
- Hoppel, W. A., G. M. Frick, J. W. Fitzgerald, and R. E. Larson, 1994: Marine boundary layer measurements of new particle formation and the effects nonprecipitating clouds have on aerosol size distribution. *J. Geophys. Res.*, **99** (D7), 14 443–14 459.
- Kazil, J., H. Wang, G. Feingold, A. D. Clarke, J. R. Snider, and A. R. Bandy, 2011: Chemical and aerosol processes in the transition from closed to open cell during VOCALS-REx. *Atmos. Chem. Phys.*, **11**, 7491–7514.
- Kleinman, L. I., and Coauthors, 2011: Aerosol concentration and size distribution measured below, in, and above cloud from the DOE G-1 during VOCALS-REx. *Atmos. Chem. Phys. Discuss.*, **11**, 17 289–17 336.
- Lance, S., A. Nenes, and R. A. Rissman, 2004: Chemical and dynamical effects on cloud droplet number: Implications for estimates of the aerosol indirect effect. *J. Geophys. Res.*, **109**, D22208, doi:10.1029/2004JD004596.
- , C. A. Brock, D. Rogers, and J. A. Gordon, 2010: Water droplet calibration of the cloud droplet probe (CDP) and in-flight performance in liquid, ice and mixed-phase clouds during ARCPAC. *Atmos. Meas. Tech.*, **3**, 1683–1706.
- Lehmann, K., H. Siebert, and R. A. Shaw, 2009: Homogeneous and inhomogeneous mixing in cumulus clouds: Dependence on local turbulence structure. *J. Atmos. Sci.*, **66**, 3641–3659.
- Lilie, L., E. Emery, J. W. Strapp, and J. Emery, 2004: A multiwire hot-wire device for measurement of icing severity, total water content, liquid water content, and droplet diameter. *Proc. 43rd AIAA Aerospace Sciences Meeting*, Reno, NV, AIAA, AIAA-2005-859.
- Meskhidze, N., A. Nenes, W. C. Conant, and J. H. Seinfeld, 2005: Evaluation of a new cloud droplet activation parameterization with in situ data from CRYSTAL-FACE and CSTRIFE. *J. Geophys. Res.*, **110**, D16202, doi:10.1029/2004JD005703.
- Nenes, A., R. J. Charlson, M. C. Facchini, M. Kulmala, A. Laaksonen, and J. H. Seinfeld, 2002: Can chemical effects on cloud droplet number rival the first indirect effect? *Geophys. Res. Lett.*, **29**, 1848, doi:10.1029/2002GL015295.
- Ramanathan, V., P. J. Crutzen, J. T. Kiehl, and D. Rosenfeld, 2001a: Aerosols, climate, and the hydrological cycle. *Science*, **294**, 2119–2124.
- , and Coauthors, 2001b: Indian Ocean Experiment: An integrated analysis of the climate forcing and effects of the great Indo-Asian haze. *J. Geophys. Res.*, **106** (D22), 28 371–28 398.
- Rosenfeld, D., U. Lohmann, G. B. Raga, C. D. O. Dowd, M. Kulmala, S. Fuzzi, A. Reissell, and M. O. Andreae, 2008a: Flood or drought: How do aerosols affect precipitation? *Science*, **321**, 1309–1313.
- , W. L. Woodley, D. Axisa, E. Freud, J. G. Hudson, and A. Givati, 2008b: Aircraft measurements of the impacts of pollution aerosols on clouds and precipitation over the Sierra Nevada. *J. Geophys. Res.*, **113**, D15203, doi:10.1029/2007JD009544.
- Small, J. D., P. Y. Chuang, G. Feingold, and H. Jiang, 2009: Can aerosol decrease cloud lifetime? *Geophys. Res. Lett.*, **36**, L16806, doi:10.1029/2009GL038888.
- Sorooshian, A., M.-L. Lu, F. J. Brechtel, H. H. Jonsson, G. Feingold, R. C. Flagan, and J. H. Seinfeld, 2007: On the source of organic acid aerosol layers above clouds. *Environ. Sci. Technol.*, **41**, 4647–4654.
- Stevens, B., and G. Feingold, 2009: Untangling aerosol effects on clouds and precipitation in a buffered system. *Nature*, **461**, 607–613.
- Strapp, J. W., and Coauthors, 2003: Wind tunnel measurements of the response of hot-wire liquid water content instruments to large droplets. *J. Atmos. Oceanic Technol.*, **20**, 791–806.
- Twohy, C. H., M. D. Petters, J. R. Snider, B. Stevens, W. Tahnk, M. Wetzel, L. Russell, and F. Burnet, 2005: Evaluation of the aerosol indirect effect in marine stratocumulus clouds: Droplet number, size, liquid water path, and radiative impact. *J. Geophys. Res.*, **110**, D08203, doi:10.1029/2004JD005116.
- Twomey, S., 1959: The nuclei of natural cloud formation, Part II: The supersaturation in natural clouds and the variation of cloud droplet concentration. *Pure Appl. Geophys.*, **43**, 243–249.
- Weber, R. J., and Coauthors, 2001: Measurements of enhanced H<sub>2</sub>SO<sub>4</sub> and 3–4 nm particles near a frontal cloud during the First Aerosol Characterization Experiment (ACE 1). *J. Geophys. Res.*, **106** (D20), 24 107–24 117.